Published in "CrystEngComm 10: 1542-1549, 2008"
which should be cited to refer to this work.

Counterion effect on the formation of coordination polymer networks between $AgNO_3$ and L (2,2′-oxybis(ethane-2,1-diyl) diisonicotinate). Part 2†

Jorge L. Sague,*[a] Markus Meuwly[b] and Katharina M. Fromm*[c]

Herein we report the synthesis and characterization by single crystal X-ray diffraction of three new silver(I) complexes $\{[Ag_2 \cdot \mathbf{L}_2](NO_3)_2(H_2O)_4\}$ (**1**), $\{[Ag_2 \cdot \mathbf{L}_2](NO_3)_2\}$ (**2**) and $\{[Ag_2 \cdot \mathbf{L}_2](NO_3)_2\}$ (**3**). Whereas compounds **2** and **3** are polymorphs, compound **1** crystallizes as the pseudo-polymorphic form of **2** and **3**. These compounds were obtained from the reaction of silver nitrate with the flexible ligand 2,2′-oxybis(ethane-2,1-diyl) diisonicotinate (**L**). The main structural motifs for complexes **1–3** are zero-dimensional metallacycles, in which two silver(I) cations are coordinated by two ligands **L** and their counterions. As a result of its unpredictable coordinating ability, the nitrate anion coordinates the Ag(I) cation in a $\mu^1\mu^2$-fashion in complex **1**, in **2** it is coordinated in an asymmetrical μ^2-mode, and in **3** the anion is strongly μ^2-symmetrical coordinating. The coordination of the NO_3^- counterions to the metal cation affects the overall supramolecular interactions in the crystalline state of the complexes (*e.g.* Ag(I)···Ag(I), π···π, hydrogen bonds and C–H···π interactions). These interactions determine the physical properties of these compounds. On heating, the crystals of compound **3** are irreversibly transformed into compound **2**. The conversion is supported by the change in the coordination mode of the nitrate counterion toward the Ag(I) cation. The solubility dependence of $AgNO_3$ in the different organic solvents used for the reactions may determine the structural diversity in the supramolecular architecture for these complexes.

Introduction

It was once claimed that: "a single grain of rice can tip the scale", meaning how subtle effects on the small microscopic scale may determine the macroscopic result. Supramolecular chemistry[1–4] is a good example of a field where small and big factors continuously interplay, effecting the outcome based on energetic factors. In this regard, one of the most important chemical phenomena is the self-recognition and the self-assembly process, which may be studied in solution or in the solid state. In the latter, the formation of crystalline species in the solid state may be analyzed by single crystal X-ray techniques, and may potentially lead to promising applications in crystal engineering.[5–11]

Nevertheless, after the self-assembly process takes place, the resulting crystalline structure is nothing but the frozen picture of all inter- or/and intramolecular interactions in equilibrium. Over the recent years, technological improvements in the measurement and detection methods in crystallography, and the development of new techniques in NMR and other analytical methods have provided a great insight into chemistry in the solid state.

From studying the role played by metal cations and ligands as the main building blocks of crystalline structures, the presence of weak interactions has emerged as a second player of extreme importance in the design of solid architectures. The importance of these weak interactions has been outlined by several authors with success, (*e.g.*, hydrogen bonds,[12–18] aromatic,[19] van der Waals,[20–23] hydrogen–ions[24] and hydrogen–aromatic interactions[25]). The control of such forces allows to some extent the construction of pre-defined arrays in the solid state.[26–31]

Whereas coordination numbers, ligand properties and solvent effects can be quite well controlled, the role of anions is often unpredictable. However, the counterion is of particular importance in the crystalline state. Together with the electrostatic relationship with metal cations, the anions may be able to generate hydrogen bonds or interact with aromatic rings. The use

[a] *University of Geneva – Sciences II, Department of Inorganic, Analytical and Applied Chemistry, 30, quai Ernest-Ansermet, CH-1211 Geneva 4, Switzerland. E-mail: Jorge.sague@chiam.unige.ch; Fax: (+41) 022 374 6409*

[b] *University of Basel, Department of Chemistry, Klingelbergstrasse 80, CH-4056, Basel, Switzerland. E-mail: m.meuwly@unibas.ch; Fax: (+41) 061 267 3855; Tel: (+41) 061 267 3821*

[c] *University of Fribourg, Department of Chemistry, Ch. Du Musee 9, CH-1700 Fribourg, Switzerland. E-mail: katharina.fromm@unifr.ch; Fax: (+41) 026 300 9738; Tel: (+41) 026 300 8732*

† For Part 1, see ref. 48.

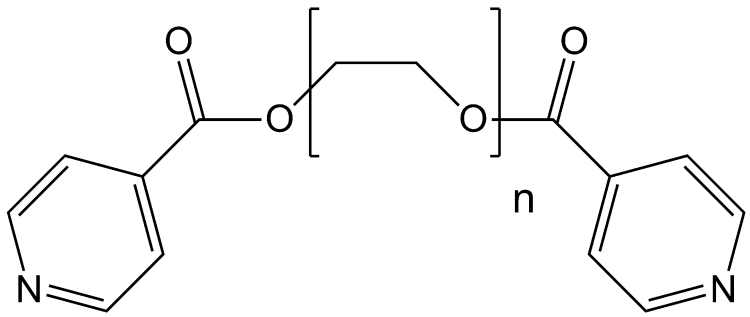

Scheme 1 Multitopic ligand used in the coordination of silver(I) salts. Increasing the ethylene glycol chain length ($n > 1$) may increase the flexibility of the ligand.

of different anions to generate diversity in the solid state has been well documented in the literature.[32,33] The results obtained are independent of the ligand employed. The formation of a particular supramolecular array may be strongly dependent on the counterion, and some examples include N-donor derived ligands containing a combination of functional groups such as pyridyl-oxadiazole,[34] pyridyl-thioether,[35,36] pyridyl-urea,[37] pyridyl-glycol[38] or pyridyl-sulfur.[39] The appropriate choice of counterion and the ligand may direct the formation of coordination networks,[40–45] discrete structures[46] or promote the cyclization of complexes in the case of silver salts.[47]

Different anions may create certain diversity in the solid state. It would be of great interest to generate different supramolecular architectures based only on the polyvalent coordinating ability of a single counterion[38] thereby influencing the chemico-physical properties.[48]

Using a "semi-rigid" ligand derived from the isonicotinic acid and polyethylene glycol (Scheme 1, $n = 1$), we reported a number of new structures.[30,31,38,48–52] Most of these compounds were infinite polymer networks arranged in layers, which were stacked through π–π, π–Ag^+ and other non-covalent interactions.

In order to study the different factors which influence the formation of a particular crystal structure, the flexibility of the chain spacer was increased ($n = 2$) and several counterion choices were tested (NO_3^-, PF_6^-, ClO_4^- and $SO_3CF_3^-$).[53] With two exceptions, (an infinite helical chain and a two-dimensional polycatenated network)[54] the obtained complexes crystallized as discrete structures, in which weak supramolecular interactions controlled the final array and dimensionality.

With the nitrate alone, three complexes were synthesized and characterized by crystallographic methods. Significant differences were observed due to the variable coordinating behavior of the counterion toward the metal cation. This behavior influences the other weak supramolecular forces present within the crystal structure conditioning the final motif in the solid state. Herein, we report the synthesis and characterization of these three new silver(I) complexes. Particular attention is paid to the role of the nitrate counterion as coordinating and polyvalent ligand for the formation of different supramolecular assemblies.

Results and discussion

When a THF solution of **L** and a water solution of silver(I) nitrate are allowed to diffuse in an H-shaped tube through a mixture of solvent ($THF : H_2O$), single crystals of the compound $\{[Ag_2 \cdot \mathbf{L}_2](NO_3)_2(H_2O)_4\}$ **1**§, are obtained in the water side of the recipient. Compound **1** crystallizes in the monoclinic space group $P2_1/n$ (No. 14). The complex lies about an inversion centre, the asymmetric unit contains a silver(I) cation coordinated by one organic ligand L, a nitrate anion and two water molecules. The ligand **L** possesses a U-shape, with two ligand molecules coordinating two silver(I) cations, generating a zero-dimensional elongated ring-like motif, a metallacycle $[Ag_2\mathbf{L}_2]^{2+}$.

The ligand **L** coordinates to the silver(I) cations through the nitrogen atoms located at the pyridine rings, with distances of Ag(1)–N(1) 2.193(3) and Ag(1)–N(2)$^{\#1}$ 2.181(3) Å. The carbonyl function remains almost parallel to the plane formed by the aromatic rings. One of the carbonyl groups on the pyridine rings is twisted with respect to the plane of the aromatic ring by −17.0(5)° (C2–C3–C6–O2) compared with −4.7(6)° for the second carbonyl group (O4–C11–C14–C13). These differences in the torsion angles may be an indication of the flexibility inherent to the spacer chain between the COO- groups.

§ Crystal data for **1**: $\{([Ag]_2[C_{16}H_{16}N_2O_5]_2)(NO_3)_2.4H_2O\}$, monoclinic, $P2_1/n$ (No. 14), $a = 13.668(3)$, $b = 7.3268(15)$ and $c = 20.232(4)$ Å, $\beta = 94.86(3)°$. $V = 2018.7(7)$ Å^3, $Z = 2$, $\delta = 1.7183(6)$ Mg m^{-3}, 4277 reflections collected, 3432 unique ($R_{int} = 0.0844$), $R_1 = 0.0454$ ($I > 2\sigma(I)$), $wR_2 = 0.0606$ (all data), CCDC 678543. Crystal data for **2**: $\{([Ag]_2[C_{16}H_{16}N_2\ O_5]_2)(NO_3)_2\}$, monoclinic, $P2_1/c$ (No. 14), $a = 6.6811(13)$, $b = 12.263(3)$ and $c = 22.585(4)$ Å, $\beta = 94.74(3)°$. $V = 1844.1(7)$ Å^3, $Z = 2$, $\delta = 1.7512(7)$ Mg m^{-3}, 3804 reflections collected, 1370 unique ($R_{int} = 0.2612$), $R_1 = 0.1237$ ($I > 2\sigma(I)$), $wR_2 = 0.2719$ (all data), CCDC 678545. Crystal data for **3**: $\{([Ag]_2[C_{16}H_{16}N_2O_5]_2)(NO_3)_2\}$ triclinic, P-1 (No. 2), $a = 6.9203(14)$, $b = 12.156(2)$ and $c = 12.332(3)$ Å, $\alpha = 63.18(3)°$, $\beta = 87.13(3)°$, $\gamma = 79.87(3)°$. $V = 910.9(3)$ Å^3, $Z = 1$, $\delta = 1.7726(8)$ Mg.m^{-3}, 3074 reflections collected, 2870 unique ($R_{int} = 0.0446$), $R_1 = 0.0386$ ($I > 2\sigma(I)$), $wR_2 = 0.0423$ (all data), CCDC 678544. The intensity data for all crystals were collected at 276 K (rt) on a Stoe IPDS II-Image Plate Diffraction System equipped with a two-circle goniometer and using Mo Kα graphite monochromated radiation. Image plate distance 140–160 mm, ω rotation scans 0–180° at f 0°, step $D_w = 1.0°$, with an exposure time of 1 min per image. The structures were solved by direct methods using the program SHELXS.[67] The refinement and all further calculations were carried out using SHELXL-97. The hydrogen atoms of the water molecules were located from Fourier difference maps. The remainder of hydrogen atoms were included in calculated positions and treated as riding atoms using SHELXL default parameters. The non-H atoms were refined anisotropically, using weighted full-matrix least-squares on F^2.

An oxygen atom (O3) of the spacer chain is disordered and was modeled and mathematically refined in two different positions (O3A and O3B with 72 and 28% occupancy). The values of torsion angles for O3A, O2–C7–C8–O3A, −54.2(5)° and O3A–C9–C10–O4, 67.7(5)° (both *gauche*), and for O3B, O2–C7–C8–O3B, −8.2(10)° and O3B–C9–C10–O4, 21.7(10)° (more *eclipse*), corroborated the preferential location of the oxygen atom at the O3A position, which may be energetically favorable.

The nitrate counterions are linked to one metal ion in a μ^2-fashion (Ag(1)–O(6), 2.747(4) and Ag(1)–O(7), 2.836(5) Å), as well as coordinating the second symmetry equivalent silver(I) cation in a monodentate manner with a distance O(7)–Ag(1)$^{\#1}$ of 2.765(5) Å. (Table 1.) Fig. 1.

Aromatic stacking interactions are relatively weak (distance of 3.763(2) Å) between metallacycles. Within the metallacycle these interactions are excluded due to the distance (5.142(2) Å). The metallacycles are stacked in a fishbone motif along the *a*-axis, and the water molecules may be directly responsible for this conformation. Indeed, water molecules are present in the crystalline structure of **1**. Two water molecules O(9) and O(10) are coordinated *via* hydrogen bonds mainly to the oxygen atom O(8) of the nitrate counter ion. This atom (O8) does not participate in the coordination toward the metal and remains "free" pointing to the inside of the cavity formed between the metallacycles (looking along the *b* axis). These water molecules and the nitrate anions form a one-dimensional helical motif based on hydrogen bonds (these helices are of alternate helicity from one helix to the next)‡ (Fig. 2).

Finally, relatively short inter-metallacycle Ag(1)···Ag(1)$^{\#2}$ interactions are present (3.3206(9) Å). The final motif for this compound is a two-dimensional architecture in the solid state.

Table 1 Most important lengths [Å] and angles [°] present in compounds **1–3**[a]

	Compound **1**	Compound **2**	Compound **3**
Ag(1)–N(1)	2.193(3)	2.189(7)	2.189(2)
Ag(1)–N(2)	2.181(3)$^{\#1}$	2.186(6)$^{\#2}$	2.175(3)$^{\#2}$
Ag(1)–O(NO_2)	2.747(4), 2.836(5), 2.765(5)$^{\#1}$	2.576(17), 2.741(16)	2.655(4), 2.650(4)
Ag(1)···Ag(1)	3.3206(9)$^{\#2}$	3.332(3)$^{\#2}$, 3.402(3)$^{\#5}$ (inter-metallacycles)	3.4339(9)$^{\#2}$
N(1)–Ag(1)–N(2)	162.86(12)$^{\#1}$	149.0(4)$^{\#2}$	151.76(9)$^{\#2}$

[a] Symmetry transformations used to generate equivalent atoms #1 $-x$, $-y$, $-z$, #2 $-x$, 1 − y, $-z$, #5 −1 − x, 1 − y, $-z$.

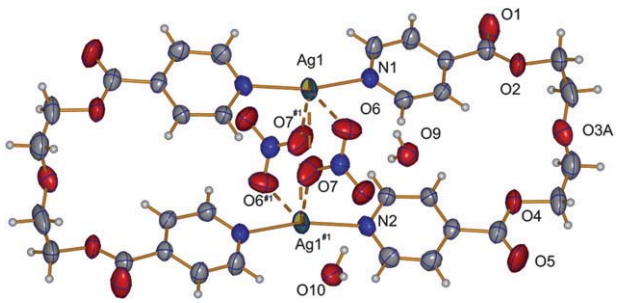

Fig. 1 Silver(I) metallacycle motif in the crystal structure of compound **1**. (Ellipsoids are represented at the 40% probability level, #1 $-x$, $-y$, $-z$.)

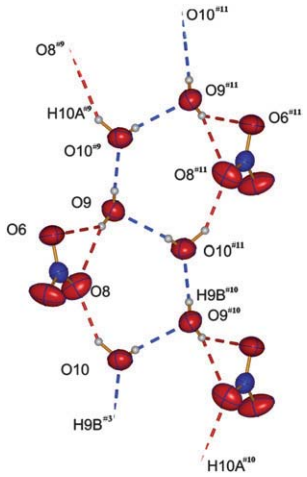

Fig. 2 Helical array formed by hydrogen bond interactions between oxygen O9 and O10 from water molecules (in dash lines, blue). These arrays are supported by additional hydrogen bond interactions with the counterion molecules (red dash lines). Ellipsoids are represented at the 40% probability level (#3 x,−1 + y, z, #9 x, 1 + y, z, #10 −1/2 − x, −1/2 + y, −1/2 − z, #11 −1/2 − x, 1/2 + y, −1/2 − z).

Single crystals of the compound {[$Ag_2 \cdot \mathbf{L}_2$](NO_3)$_2$} **2**§ were collected from the side of the H-tube where the ligand was initially dissolved (THF). In this compound, no water molecules are found in the structure. Compound **2** crystallizes in the monoclinic space group $P2_1/c$ (No. 14). The asymmetric unit possesses one Ag(I) cation, one nitrate counterion and one ligand **L**, the last two are coordinating to the silver atom, the dimer complex formed lies about an inversion centre.

Like in the previous compound **1**, the ligand in **2** possesses a U-shape conformation, forming a [$Ag_2\mathbf{L}_2$]$^{2+}$ metallacycle.

Distances Ag(1)–N are in the usual range (2.189(6), Ag(1)–N(1) Å and 2.186(6), Ag(1)–N(2)$^{\#2}$ Å) for this type of compound. The angle N(1)–Ag(1)–N(2) is, however, distorted (149.0(4)°). The strong interaction between the silver cation and the nitrate counterion may be responsible for this effect (Table 1). One nitrate coordinates to one silver atom in an asymmetric μ^2-fashion (2.576(16), Ag(1)–O(6) Å and 2.741(16), Ag(1)–O(7) Å), providing thus a distorted T-shape coordination motif for the metal atom (Fig. 3).

Regarding the ligand **L**, the carbonyl group remains in the same plane as the pyridine ring. The metallacycle in **2** is slightly more elongated (17.5 Å in **2** *versus* 17.3 Å in **1**), and the ring will consequently decrease. As in compound **1**, the oxygen atom O3

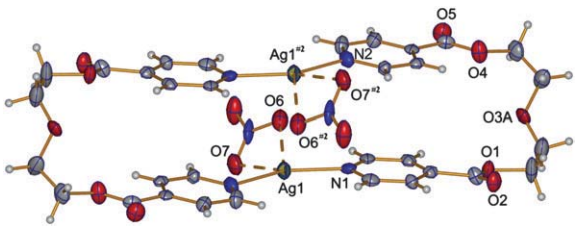

Fig. 3 Silver(I) metallacycle motif present in the crystal structure of compound **2** (Ellipsoids are represented at the 16% probability level. #2 $-x$, 1 − y, $-z$.)

of **2** located in the spacer chain is disordered and occupies two different positions (70%, O3A and 30%, O3B). The torsion angles in the polyether chain are for O3A, 36(4)° (O2–C7–C8–O3A) and 75(2)°, O3A–C9–C10–O4 and for O3B, 88(3)° (O2–C7–C8–O3B) and 11(5)°, O3B–C9–C10–O4. This difference in the elongation of the di-ethylene glycol spacer in **2**, implies a distortion of about 30.8° on the intrametallacycle pyridine–pyridine stacking.

Short intra- and inter-metallacycle Ag···Ag distances are present, with 3.332(3)$^{\#2}$ and 3.402(3)$^{\#5}$ Å, respectively. These metal–metal contacts may induce the pyridine rings to share a common axis, which crosses the two silver cations within one metallacycle. This may be responsible for the significant distortion of the metallacycle in **2**. The presence of π–π aromatic stacking interactions is excluded due to the distance (4.007(7) Å between ring centroids). The metallacycles are stacked forming columns parallel to each other along the *b* axis. They possess an undulated form along the *c* axis.

Single crystals of compound $\{[Ag_2 \cdot \mathbf{L}_2](NO_3)_2\}$ **3**§, grew when two DMSO solutions of ligand **L** and silver nitrate were mixed together. Compounds **2** and **3** are polymorphs, differing significantly in the coordination mode of the nitrate counterion toward the metal cation. Compound **3** crystallizes in the solid state in the triclinic system, space group *P*-1 (No. 2). The asymmetric unit contains a silver cation coordinated by a ligand **L** and a nitrate counterion, in a fashion similar to compound **2** and, as in compound **2**, the dimer complex lies about an inversion centre.

In compound **3**, each nitrate anion coordinates to one silver cation in an almost quasi perfect symmetrical bidentate mode (Ag(1)–O(7), 2.650(4) Å and 2.655(4) Å, Ag(1)–O(6)) (Fig. 4).

Each silver(I) cation is linked furthermore by two pyridine rings to form a distorted tetrahedral motif around the metal atom (Ag(1)–N(1), 2.189(2) Å and 2.175(3) Å, Ag(1)–N(2)$^{\#1}$). The angle N(1)–Ag(1)–N(2) is 151.76(9)° (Table 1).

The carbonyl group remains in the plane of the aromatic ring (O1–C6–C3–C4, 3.6(6)° and O4–C11–C14–C13, −2.0(4)°) and points to the outer side (exo) of the surface that contains the aromatic ring. In the diethylene glycol spacer the oxygen atom O3 is disordered (occupancy 75% for O3A and 25% for O3B) but differs from **1** and **2**, both disordered positions possess a "*gauche*" type conformation with torsion angles for O3A of 47.2(6)° (O2–C7–C8–O3A) and −80.3(4)° (O3A–C9–C10–O4), whereas for O3B, they are −28.6(10)° (O2–C7–C8–O3B) and −32.1(7)° (O3B–C9–C10–O4). The angle between the planes crossing the pyridine rings is 9.6(8)°, which shows a slight bending and asymmetry in the ring stacking. In compound **3**, π–π interactions are present, which are strongest in the inter-metallacycle region (3.873(2) Å).

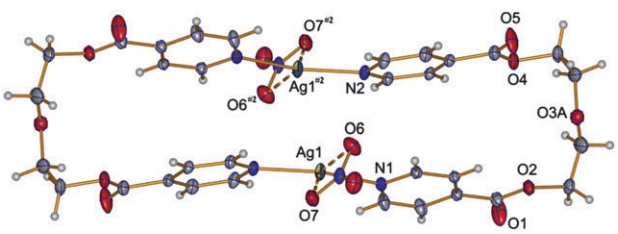

Fig. 4 Silver(I) metallacycle motif present in the crystal structure of compound **3** (Ellipsoids are represented at the 16% probability level. #2 $-x, 1-y, -z$.)

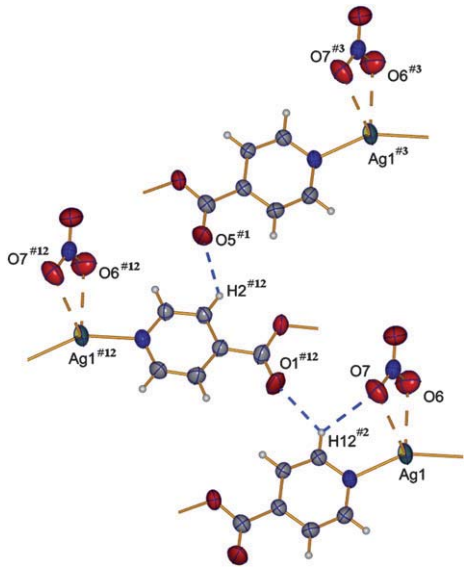

Fig. 5 Main hydrogen bond motif present in compound **3**. The interaction between the oxygen atoms O1, O7 and O5 and the hydrogen atoms H12 and H2, respectively, generate a two-dimensional network. Further interactions present in the crystal structure increase the dimensionality from 2D to 3D. (Ellipsoids are represented at the 50% probability level, #1 $-x, -y, -z$, #2 $-x, 1-y, -z$, #3 $x, -1+y, z$, #12 $x, y, -1+z$.)

Weak intra-metallacycle Ag(I)···Ag(I) interactions are present, and are longer than the Ag(1)···Ag(1) contacts between the silver atoms from adjacent metallacycles (3.4339(9)$^{\#2}$ Å and 3.648(3)$^{\#7}$ Å respectively, #7 $1-x, 1-y, -z$). The aromatic pyridine rings of the same ligand are twisted by 28.5(2)° from the axis formed by the intra metallacycle Ag···Ag axis.

As found frequently in the solid state, the distance C1–H1··· centroid (aromatic ring) is ∼3.18 Å, suggesting a C–H···π interaction.[19] However, in the presence of this interaction, Ag··· Ag and π···π stacking should act in a synergistic manner. Hydrogen bonds formed by the oxygen atom of the carbonyl group of **L**, the oxygen atoms of the nitrate counterion and the hydrogen atoms of the pyridine rings generate a three-dimensional network in the solid state‡ (Fig. 5).

Counterion role in the crystalline state of compounds 1–3

Complexes **1**, **2** and **3** possess the same crystal morphology and crystallize as prism-type crystals. While compounds **2** and **3** are polymorphs, all three compounds (**1–3**) may be considered network isomers, as the water present in **1** does not affect the overall array. Indeed, after removing the water, the structure does not suffer structural decomposition as was confirmed by TG/SDTA experiments.

In these compounds the polyvalence of the nitrate counterions as strong coordinating anions toward the silver(I) cations is expressed in different manners: in compound **1** it does so in a μ^2–μ^1 fashion, coordinating two silver atoms from the same metallacycle (Ag(1)–O(6), 2.747(4) Å; Ag(1)–O(7), 2.836(5) Å), and O(7)$^{\#1}$–Ag(1), 2.765(5) Å). Weak exo-ring metal–metal contacts (Ag(1)···Ag(1)$^{\#2}$, 3.3206(9) Å) are present and generate a distorted square planar pyramid coordination around the metal atom.

The monodentate coordination of the NO_3^- in **2** is unusual. Nitrate anions with three potential coordinating oxygen atoms, more often bind in a bidentate fashion. Only a few monodentate nitrate coordinating anions have been reported so far.[55] In **2**, the second closest oxygen atom to the silver(I) atom is at 2.741(16) Å (Ag(1)–O(7)), compared to the 2.576(16) Å for Ag(1)–(O6). This coordination bond may not be relevant for the coordination sphere of the silver cation.

The presence of such a strong coordination and consequently the charge density decrease on the silver atoms probably induces in **2** some weak intermetallic interactions (endo- and exo-metallacycle distances Ag(1)···Ag(1), 3.33(3)$^{\#2}$ and 3.402(3)$^{\#5}$, respectively). The nitrate molecules are partially included in the region delimited by the metallacycle. In compound **3**, however, the counterion is displaced from the volume formed by one metallacycle and occupies instead the space in-between two different metallacycles. In **3**, the nitrate coordinates the metal cation almost as strongly as in **2**, and in a symmetrical-bidentade pincer fashion with distances Ag(1)–O(7), 2.650(4) Å and 2.655(4) Å for Ag(1)–O(6). Some weak Ag···Ag interactions are thus also present in **3**. These interactions are endo- and exo-metallacycles (*endo* Ag(1)···Ag(1)$^{\#2}$, 3.4339(9) and *exo* Ag(1)···Ag(1)$^{\#7}$, 3.648(3) Å), again a possible result of the strong counterion coordination to the metal cation (Fig. 6).

Strong coordinating counterions like nitrates, which are potential hydrogen bond acceptors, enhance the probable presence of water molecules in similar supramolecular compounds within the crystalline structure.[49,56] In compound **1**, a helical array of water molecules is present. These water molecules do not interact directly with the silver cation or the ligand **L**, but the interaction with the nitrate counterion does affect the overall crystalline packing.

The role of the water molecules directing the supramolecular array of one particular compound has been well established.[57–59] Particularly, water nanowires have been found in porous structures formed by calixarenes and their derivatives, which are suitable scaffolds for such arrays.[60] Discrete water clusters (formed by 4 water molecules in a plane) are more rare, although these were recently observed in an example of a silver(I) metallacycle.[61] This type of array is strongly stabilized by the presence of hydrogen bonds with the organic ligands. If such interactions are present we may envisage the elongation in the direction perpendicular to the plane formed by the water molecules to generate a helical array.

To evaluate the role of the water molecules in the crystal structure of compound **1**, TG/DSC measurements were performed on single crystals. The results show a quantitative loss of water at 120 °C and decomposition of the sample at 202 °C. A difference compared with other reported compounds that possess a reversible system containing water, is that compound **1** does not collapse when water is removed thermally from the channel.[62] In complex **1**, the thermal removal of water does not lead to chemical decomposition.

Inter-conversion between the hydrated and the dehydrated structure has been tested under thermal conditions for several compounds.[63] In the case of **1**, the dehydration is an irreversible process.

The coordination mode observed for the NO_3^- anion towards the silver(I) cation may be responsible for the packing in the solid state of these compounds. In **1**, the presence of the water helix in the cavity formed by metallacycles and the counterions elongates the distances between parallel rings (Ag–Ag, ~13.5 Å). At the same time, it causes the twist of the metallacycles to the inside of the cavity (Fig. 7a). An Ag–Ag distance of ~12.9 Å is observed in **2**, compared to the shorter distance (~12.1 Å) in **3** (Fig. 7b, c).

This variation in distances may depend on whether the counterion coordinates in a μ^1-fashion (as in **1**) or in a weak to strong μ^2-fashion (like **2** and **3**), with the μ^2-mode occupying less volume thus making the crystalline packing more compact.

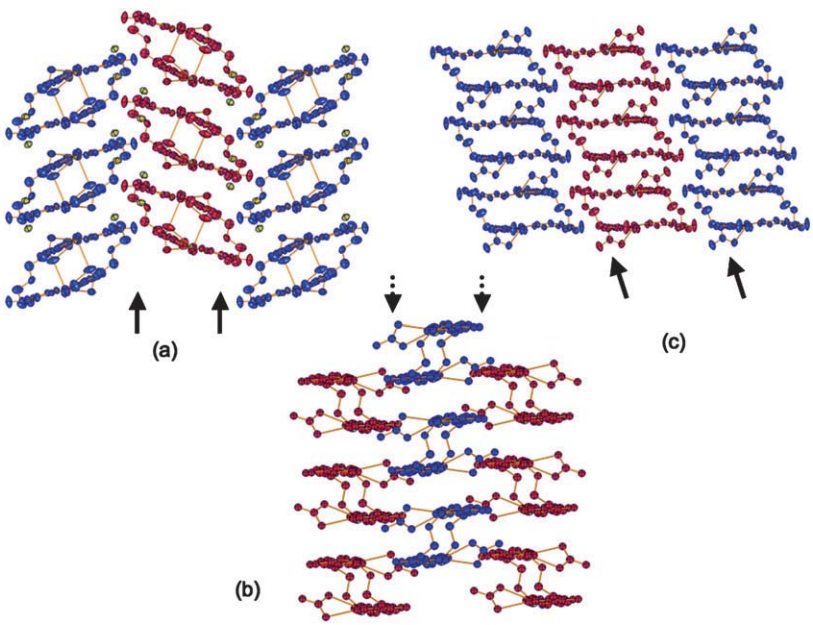

Fig. 6 Metallacycle stacking in the crystal structure of compound **1–3**. The arrows are pointing to the position of the counterions along the crystal packing. the metallacycles stacked columns are slightly displaced (represented in red and blue); (a) view along the *a* direction in compound **1**, the packing is distorted due to the presence of water molecules (yellow dots) and the interaction between these molecules and the NO_3^- counterions; (b) view along the [2, 0, 31] direction in compound **2**, the parallel stacked columns are slightly displaced; (c) view along the *c* direction in compound **3**.

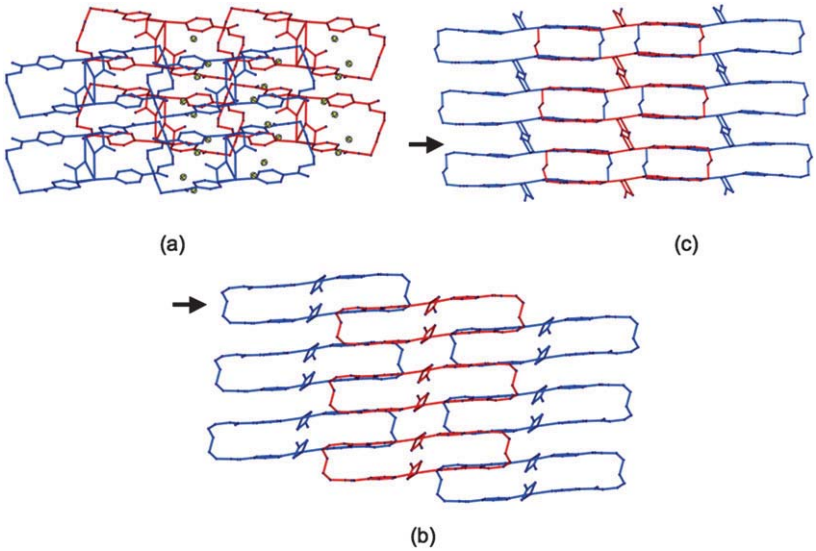

Fig. 7 Counterion coordination and metallacycle stacking in the crystal structure of compound **1–3**. (a) View along the *c* direction in compound **1**, the interactions between the water molecules (yellow dots) and the NO_3^- counterion molecules generate two different directions in the crystalline packing; (b) view along the *b* direction in compound **2**, the counterion molecules are contained in the layers formed by the metallacycles (black arrow), the metallacycles stacked columns are slightly displaced (represented in red and blue); (c) view along the *b* direction in compound **3**, the counterion molecules are located between the layers formed by the metallacycles (black arrow).

TG/SDTA experiments show that compounds **1**, **2** and **3** melt at different temperatures. This allowed us to identify three isomers not just only in the crystalline state, but also when polycrystalline or amorphous samples were obtained.

When single crystals of complex **3** were warmed (80 °C) for a week, the complex interconverted to compound **2**, where the nitrate counterion coordinates in a monodentate mode to the silver(I) cation. The dependence of the coordination ability of the nitrate counterion upon heating has been studied since 1996.[64] In compounds **2** and **3** this process is time and temperature dependent. The conversion of compound **3** to compound **2** does not take place in a short period of time (a few days) and heating over 80 °C destroys the crystallinity of the sample. The time required for this interconversion limited the use of the TG/SDTA technique to follow the process.

Theoretical calculations on compounds 1–3

DFT calculations at the B3LYP/6–311++G** level were carried out to estimate the stabilization energy due to ligand **L** in the metallacycles. The crystallographic coordinates of the organic ligand were extracted from the crystal structures of **L** : Ag complexes ($\mathbf{L}_c$) and used in the theoretical model without further optimization. The calculated value from the crystallographic data of the crystal structure of the ligand **L** ($\mathbf{L}_l$) was used as a reference. All data obtained are expressed as the difference between $\mathbf{L}_l$ and $\mathbf{L}_c$.

The results obtained show the total energy ($\triangle E_t$), the energy due to the $\pi\cdots\pi$ interactions ($\triangle E_r$) and stabilization energy due to the diethylene glycol conformation ($\triangle E_\tau$) (Table 2).

As expected, the $\triangle E_r$ may depend on the distance between the aromatic ring centroids and the position at which the pyridine rings are stacked.

Approaching the centroids of the two aromatic rings may increase the repulsion between the aromatic electrons. This is proportional to the values found for $\triangle E_r$. The increase of energy is maximal at a distance of 4.149(8)Å (+3.00 kcal mol^{-1}, compound **3**) and then drops to 4.082(9) Å (−7.22 kcal mol^{-1}, compound **2**).

Table 2 DFT calculation results for the ligand in the metallacycles[a]

Compound	$\triangle E_t$	π–π/Å	$\triangle E_r$	$\triangle E_\tau$
Ligand **L**	—	5.801(6)	—	—
1	+9.99	5.142(6)	−7.22	+16.46
2	+20.07	4.082(9)	−5.12	+25.42
3	+74.14	4.149(8)	+3.00	+68.72

[a] All calculated energies are given in kcal mol^{-1}.

Concerning the spacer chain, the torsion angles of compounds **2** and **3** are relatively strained compared to the values found in **1**. This fact may in part explain the energy difference found in the calculations. This strain significantly destabilizes the metallacycle in both compounds **2** and **3** compared to compound **1**.

The $\triangle E_t$ was calculated without taking into account the ligand-to-silver(I) and silver(I)-to-counterion interactions in the metallacycle. Thus, this result concerns only the ligand part of the ring, and it is noteworthy that the value of $\triangle E_t$ is approximately equal to ($\triangle E_r$ + $\triangle E_\tau$).

The structural change of compound **3** to **2**, where the silver(I) cation is asymmetrically coordinated by the nitrate counterion agrees with the plausible gain in energy for the ligand when changing from **3** to **2** (about +54 kcal mol^{-1}). However, previous calculations on the metallacycles of **2** and **3**, without considering the counterion, show the opposite result. In that case the metallacycle in **3** seems to be energetically more stable than the metallacycle in **2**. The theoretical effect of the counterion in both structures is currently under investigation and the results may determine the reason for this interconversion process.

The solvent is another factor to be carefully analyzed. Solvent polarity may indirectly promote the crystalline self-assembly of compounds **1–3**. By analyzing by ES-MS spectrometry samples prepared in THF/water in variable proportions and DMSO we were able to assess the presence of the metallacycle complex in solution ($\{[Ag(\mathbf{L}1)]_2NO_3\}^+$, 910 *m*/*z*), but after increasing the concentration of the ligand, new polymeric species begin to appear and become dominant in the spectra‡.

Although the presence of different compounds was evident from ES-MS, the collection of single crystals from different batches where several crystallization techniques were used afforded only compounds **1–3**.

The same results were obtained after changing the concentration of the reactants. This may be an indication that the crystallization process of the metallacycles is thermodynamically controlled yielding only metallacycles when the system is undisturbed.

After being formed complexes **1–3** are remarkably stable. Some assays to exchange NO_3^- counterions for others counterions ($SO_3CF_3^-$, PF_6^-, ClO_4^-) were carried out without success. The crystals of complexes **1–3** remain stable under daylight for several months. This phenomenon has been reported in a recent publication.[65]

Conclusions

Three supramolecular assemblies with silver(I) nitrate and a flexible organic ligand (**L**) were synthesized, two of these compounds are polymorphs (**2** and **3**) whereas compound **1** crystallizes as the hydrated form of **2** and **3** and may be considered a pseudo-polymorphic form of these compounds. The coordinating mode of the nitrate anion to the silver(I) ions varies from $\mu^2\mu^1$—in compound **1**, μ^1—in compound **2** to a μ^2—symmetrical bidentade coordination in compound **3**. These flexible coordination modes enable the stacking of the metallacycles in the solid state in column arrays, where aromatic and metal-to-metal interactions are present. The availability of free oxygen atoms, which may remain non-coordinating, allow the formation of various hydrogen bonding networks. These may control the interactions between the columns of stacking metallacycles, and thus, the final supramolecular motif in the solid state. The stronger bonding anion–cation may affect other weak supramolecular forces (like metal-to-metal interactions), varying the chemico-physical properties of such complexes in the solid state.

The synthesis and characterization of complexes **1–3** enable the investigation of the structural diversity inherent to the polyvalent coordination ability of a single counterion. The extension of this work to a similar type of supramolecular systems may be fundamental to the study of the bonding interactions present in the solid state.

Experimental

The synthesis of ligand **L** has been previously reported.[66]

Synthesis of compounds $\{[Ag_2\cdot L_2](NO_3)_2(H_2O)_4\}$ (1), $\{[Ag_2\cdot L_2](NO_3)_2\}$ (2) and $\{[Ag_2\cdot L_2](NO_3)_2\}$ (3)

Crystals suitable for single X-ray diffraction were grown after slow diffusion of **L** (30 mg, 0.094 mmol) dissolved in THF (5 mL), through a mixture of water : THF 1 : 5, into a solution of water (5 mL) containing $AgNO_3$ (16.3 mg, 0.094 mmol).

The crystals taken from the silver side afforded complex **1** (hydrated). The crystals, which grew in the ligand side showed the presence of complex **2**, where the absence of water was remarkable.

Yields (**1**): 19.9 mg (0.037 mmol, 40% calculated with respect to $AgNO_3$). Elemental analysis: calculated: C 36.78, H 3.86, N 8.05%; found: C 36.7, H 3.8, N 8.1%. IR: ν(Ar–H) 3067.4 s, ν(–HC–H) 2910.0 s, ν(C=O) 1721.9 s, ν(C=C) 1548.9 w, ν(ArC–C, C=N) 1423.6 w, ν (NO_3) 1375.9–1273.7 s, ν(–C–O) 1116.3 s, ν(ArC–H) 691.9 m

Yields (**2**): 13.8 mg (0.028 mmol, 30% calculated with respect to $AgNO_3$). Elemental analysis: calculated: C 39.51, H 3.32, N 8.64%; found: C 38.7, H 3.3, N 8.60%. IR: ν(Ar-H) 3022.3 s, ν(–HC–H) 2919.2 s, ν(C=O) 1715.0 s, ν(ArC–C, C=N) 1412.1 w, ν(NO_3) 1362–1230.0 s, ν(–C–O) 1124.1 s, ν(ArC–H) 690.5 m

Synthesis of compound $\{[Ag(L)]NO_3\}_2$ (3)

L (60 mg, 0.18 mmol) was reacted with $AgNO_3$ (32 mg, 0.18 mmol) in DMSO (15 mL). The solution was left in the dark for 1 month. Transparent single crystals suitable for X-ray diffraction were collected. The crystals were filtered off and complex **3** was measured.

Yields (**3**): 56.8 mg (0.11 mmol, 65% calculated with respect to $AgNO_3$). Elemental analysis: calculated: C 39.51, H 3.32, N 8.64%; found: C 39.5, H 3.30, N 8.62%. IR: ν(Ar-H) 3050.0 s, ν(-HC–H) 2925.2 s, ν(C = O) 1720.3 s, ν(ArC–C, C = N) 1414.0 w, ν(NO_3) 1373–1228.3 s, ν(-C–O) 1126.3 s, ν(ArC–H) 694.3 m

Acknowledgement

The authors thank the Swiss National Foundation for their most generous support.

References

1 M. Albrecht, *Naturwissenschaften*, 2007, **94**, 951–966.
2 K. Gloe, K. Gloe, H. Hesske and L. F. Lindoy, *Wiss. Z. Tech. Univ. Dresden*, 2007, **56**, 32–38.
3 F. Diederich, *Angew. Chem., Int. Ed.*, 2007, **46**, 68–69.
4 M. Albrecht, *Nachr. Chem.*, 2004, **52**, 290–291.
5 G. R. Desiraju, *Angew. Chem., Int. Ed.*, 2007, **46**, 8342–8356.
6 C. B. Aakeroy and A. M. Beatty, *Compr. Coord. Chem. II*, 2004, **1**, 679–688.
7 D. Braga, *Chem. Commun.*, 2003, 2751–2754.
8 C. Janiak, *Dalton Trans.*, 2003, 2781–2804, (and references herein).
9 E.-C. Yang, J. Li, B. Ding, Q.-Q. Liang, X.-G. Wang and X.-J. Zhao, *CrystEngComm*, 2008, **10**, 158–161.
10 G.-B. Che, C.-B. Liu, B. Liu, Q.-W. Wang and Z.-L. Xu, *CrystEngComm*, 2008, **10**, 184–191.
11 Q.-B. Bo, Z.-X. Sun and W. Forsling, *CrystEngComm*, 2008, **10**, 232–238.
12 T. N. Pham, J. M. Griffin, S. Masiero, S. Lena, G. Gottarelli, P. Hodgkinson, C. Filip and S. P. Brown, *Phys. Chem. Chem. Phys.*, 2007, **9**, 3416–3423.
13 C. J. Adams, H. M. Colquhon, P. C. Crawford, M. Lusi and A. G. Orpen, *Angew. Chem., Int. Ed.*, 2007, **46**, 1124–1128.
14 D. Braga, S. L. Giaffreda, K. Rubini, F. Grepioni, M. R. Chierotti and R. Gobetto, *CrystEngComm*, 2007, **9**, 39–45.
15 A. Cammers and S. Parkin, *CrystEngComm*, 2004, **6**, 168–172.
16 T. Steiner, *Crystallogr. Rev.*, 2003, **9**, 177–228.
17 T. Steiner, *Angew. Chem., Int. Ed.*, 2002, **41**, 48–76.
18 K. M. Fromm, *Chem.–Eur. J.*, 2001, **7**, 2236–2244.
19 C. Janiak, *J. Chem. Soc., Dalton Trans.*, 2000, 3885–3896.

20 F. Lerouge, G. Cerveau and R. J. P. Corriu, *New J. Chem.*, 2006, **30**, 1364–1376.
21 B. Gong, C. Zheng, E. Skrzypczak-Jankun and J. Zhu, *Org. Lett.*, 2000, **2**, 3273–3275.
22 F. Hajek, E. Graf, M. W. Hosseini, A. De Cian and J. Fischer, *Cryst. Eng.*, 1998, **1**, 79–85.
23 O. F. Devereux and P. L. De Bruyn, *J. Chem. Phys.*, 1962, **37**, 2147–2148.
24 D. Braga, L. Maini, M. Polito and F. Grepioni, *Struct. Bonding*, 2004, **111**, 1–32.
25 M. Nishio, *CrystEngComm*, 2004, **6**, 130–158.
26 E. Bukhaltsev, I. Goldberg, R. Cohen and A. Vigalok, *Organometallics*, 2007, **26**, 4015–4020.
27 C. M. Reddy, L. S. Reddy, S. Aitipamula, A. Nangia, C.-K. Lam and T. C. W. Mak, *CrystEngComm*, 2005, **7**, 44–52.
28 P. Sozzani, A. Comotti, S. Bracco and R. Simonutti, *Chem. Commun.*, 2004, 768–769.
29 T. Yajima, G. Maccarrone, M. Takani, A. Contino, G. Arena, R. Takamido, M. Hanaki, Y. Funahashi, A. Odani and O. Yamauchi, *Chem.–Eur. J.*, 2003, **9**, 3341–3352.
30 K. M. Fromm, *Kirk-Othmer Encycl. Chem. Technol. (5th Ed.)*, 2004, **7**, 573–606.
31 A. Y. Robin and K. M. Fromm, *Coord. Chem. Rev.*, 2006, **250**, 2127–2157, (and references herein).
32 J.-Y. Cheng, Y.-B. Dong, R.-Q. Huang and M. D. Smith, *Inorg. Chim. Acta*, 2005, **358**, 891–902.
33 Y.-B. Dong, J.-Y. Cheng, R.-Q. Huang, M. D. Smith and H.-C. Zur Loye, *Inorg. Chem.*, 2003, **42**, 5699–5706.
34 G. Mahmoudi and A. Morsali, *CrystEngComm*, 2007, **9**, 1062–1072.
35 X.-H. Bu, Y.-B. Xie, J.-R. Li and R.-H. Zhang, *Inorg. Chem.*, 2003, **42**, 7422–7430.
36 Y.-B. Xie and X.-H. Bu, *J. Cluster Sci.*, 2004, **14**, 471–482.
37 D. R. Turner, B. Smith, E. C. Spencer, A. E. Goeta, I. Radosavljevic Evans, D. A. Tocher, J. A. K. Howard and J. W. Steed, *New J. Chem.*, 2005, **29**, 90–98.
38 A. Y. Robin, J. L. Sague Doimeadios, A. Neels, T. Vig Slenters and K. M. Fromm, *Inorg. Chim. Acta*, 2007, **360**, 212–220.
39 D. M. L. Goodgame, D. A. Grachvogel, S. Holland, N. J. Long, A. J. P. White and D. J. Williams, *J. Chem. Soc., Dalton Trans.: Inorg. Chem.*, 1999, 3473–3481.
40 O. V. Dolomanov, D. B. Cordes, N. R. Champness, A. J. Blake, L. R. Hanton, G. B. Jameson, M. Schroeder and C. Wilson, *Chem. Commun.*, 2004, 642–643.
41 A. J. Blake, N. R. Champness, S. M. Howdle, K. S. Morley, P. B. Webb and C. Wilson, *CrystEngComm*, 2002, **4**, 88–92.
42 A. N. Khlobystov, A. J. Blake, N. R. Champness, D. A. Lemenovskii, A. G. Majouga, N. V. Zyk and M. Schroder, *Coord. Chem. Rev.*, 2001, **222**, 155–192.
43 M. A. Withersby, A. J. Blake, N. R. Champness, P. A. Cooke, P. Hubberstey, W.-S. Li and M. Schroder, *Cryst. Eng.*, 1999, **2**, 123–136.
44 A. J. Blake, N. R. Champness, S. M. Howdle and P. B. Webb, *Inorg. Chem.*, 2000, **39**, 1035–1038.
45 A. J. Blake, N. R. Brooks, N. R. Champness, M. Crew, D. H. Gregory, P. Hubberstey, M. Schroder, A. Deveson, D. Fenske and L. R. Hanton, *Chem. Commun.*, 2001, 1432–1433.
46 D. A. Beauchamp and S. J. Loeb, *Chem. Commun.*, 2002, 2484–2485.
47 O.-S. Jung, Y.-A. Lee, Y. J. Kim and J. Hong, *Cryst. Growth Des.*, 2002, **2**, 497–499.
48 A. Y. Robin, J. L. Sague and K. M. Fromm, *CrystEngComm*, 2006, **8**, 403–416.
49 A. Y. Robin, M. Meuwly, K. M. Fromm, H. Goesmann and G. Bernardinelli, *CrystEngComm*, 2004, **6**, 336–343.
50 A. Y. Robin, K. M. Fromm, H. Goesmann and G. Bernardinelli, *CrystEngComm*, 2003, **5**, 405–410.
51 K. M. Fromm, E. D. Gueneau, A. Y. Robin, W. Maudez, J. Sague and R. Bergougnant, *Z. Anorg. Allg. Chem.*, 2005, **631**, 1725–1740.
52 K. M. Fromm, *Abstracts of Papers, 232nd ACS National Meeting, San Francisco, CA, US*, Sept 10–14 2006 INOR-023.
53 K. M. Fromm and J. L. Sague, will be published elsewhere.
54 J. L. Sague and K. M. Fromm, *Cryst. Growth Des.*, 2006, **6**, 1566–1568.
55 S. O. Sommerer, B. L. Westcott, A. J. Jircitano and K. A. Abboud, *Inorg. Chim. Acta*, 1995, **238**, 149–153.
56 G. A. Bowmaker, Effendy, K. C. Lim, B. W. Skelton, D. Sukarianingsih and A. H. White, *Inorg. Chim. Acta*, 2005, **358**, 4342–4370.
57 R. Pomes and B. Roux, *Biophys. J.*, 2002, **82**, 2304–2316.
58 M. O. Jensen, U. Rothlisberger and C. Rovira, *Biophys. J.*, 2005, **89**, 1744–1759.
59 J. Mann David and D. Halls Mathew, *Phys. Rev. Lett.*, 2003, **90**, 195503.
60 Y. Liu, D.-S. Guo and H.-Y. Zhang, *J. Mol. Struct.*, 2005, **734**, 241–245.
61 L. S. Yue Nancy, C. Jennings Michael and J. Puddephatt Richard, *Inorg. Chem.*, 2005, **44**, 1125–1131.
62 B. Lou, F. Jiang, D. Yuan, B. Wu and M. Hong, *Eur. J. Inorg. Chem.*, 2005, 3214–3216.
63 J. J. Vittal and X. Yang, *Cryst. Growth Des.*, 2002, **2**, 259–262.
64 A. Katrusiak and M. Szafranski, *J. Mol. Struct.*, 1996, **378**, 205–223.
65 T. Dorn, K. M. Fromm and C. Janiak, *Aust. J. Chem.*, 2006, **59**, 22–25.
66 K. M. Fromm, J. L. S. Doimeadios and A. Y. Robin, *Chem. Commun.*, 2005, 4548–4550.
67 G. M. Sheldrick, *Crystallogr. Comput.: Data Collect., Struct. Determ., Proteins, Databases, Pap. Int. Summer Sch., 9th*, 1985, 184–189.